UNIVERSITY OF LEEDS

This is a repository copy of *Organic and Third Phase in HNO3/TBP/n-Dodecane System: No Reverse Micelles*.

White Rose Research Online URL for this paper:
http://eprints.whiterose.ac.uk/120285/

Version: Accepted Version

THE ORGANIC AND THE THIRD PHASE IN THE SYSTEM HNO₃/TBP/n-DODECANE: NO REVERSE MICELLES

*P. Ivanov,[a] J. Mu,[b] L. Leay,[b,c] S.-Y. Chang,[b,d] C. A. Sharrad,[b,c] A. J. Masters,[b] S. L. M. Schroeder,[b,d,e]

[a]National Physical Laboratory, Hampton Road, Middlesex, TW11 0LW Teddington, UK

[b]School of Chemical Engineering and Analytical Science, University of Manchester, M13 9PL, UK

[c]Research Centre for Radwaste and Decommissioning, Dalton Nuclear Institute, University of Manchester, M13 9PL, UK

[d](Present address) Diamond Light Source Ltd., Didcot, Oxfordshire, OX11 0DE, UK

[e](Present address) School of Chemical and Process Engineering, University of Leeds, Leeds LS2 9JT, UK

The composition and speciation of the organic and third phases in the system HNO₃/TBP/n-dodecane have been examined by a combination of gravimetry, Karl Fischer analysis, chemical analysis, FTIR and ^{31}P NMR spectroscopy, with particular emphasis on the transition from the two-phase to the three-phase region. Phase densities indicate that third phase formation takes place for initial aqueous HNO_3 concentrations above 15 M, whilst the results from the stoichiometric analysis imply that the organic and third phases are characterized by two distinct species, namely the mono-solvate TBP·HNO₃ and the hemi-solvate TBP·2HNO₃, respectively. Furthermore, the ^{31}P-NMR spectra of organic and third phase show no significant chemical differences at the phosphorus centres, suggesting that the second HNO_3 molecule in the third phase is bound to HNO_3 rather than TBP. The third phase FTIR spectra reveal stronger vibrational absorption bands at 1028, 1310, 1653 and 3200-3500 cm⁻¹, reflecting higher concentrations of H_2O, HNO_3 and TBP. The molecular dynamics simulation data predict structures in accord with the spectroscopically identified speciation, indicating inequivalent HNO_3 molecules in the third phase. The predicted structures of the organic and third phases are more akin to microemulsion networks rather than the distinct, reverse micelles assumed in previous studies. H_2O appears to be present as a disordered hydrogen-bonded solvate stabilising the

28   polar TBP/HNO₃ aggregates in the organic matrix, and not as a strongly bound hydrate species in

29   aggregates with defined stoichiometry.

30

33

34   *Correspondence: peter.ivanov@npl.co.uk

35

INTRODUCTION

37   The principal method for reprocessing of spent nuclear fuel is the PUREX (Plutonium URanium

38   EXtraction) process, which is based on solvent extraction of the two actinide elements from nitric acid

39   solutions by tri-n-butyl phosphate (TBP), dissolved in either odourless kerosene or the aliphatic

40   hydrocarbon n-dodecane.[1] Extraction systems built on such organophosphorus ligands dissolved in

41   aliphatic solvents can suffer from third phase formation, when threshold concentrations of extracted

42   metal and/or acid are exceeded. Such third phase formation is exhibited also by N-based extractants

43   such as amides, as well as tetraalkylammonium salts and amines. [2-5] Third phase formation is readily

44   recognisable as a separate, dense organic phase enriched in extractant, acid and metal relative to the

45   lighter organic phase. Formation of third phase is an undesirable process in the reprocessing of spent

46   fuel, as it could potentially cause safety and even criticality concerns due to the high metal

47   concentrations and can lead to phase inversion issues. [6] Third phase formation is often considered to

48   be the result of limited solubility of metal-ligand complexes in the organic medium, so that the

49   colloidal suspension formed by TBP acting as a surfactant becomes favourable at higher metal

50   loadings. [7, 8] The phase splitting process in a variety of TBP-based systems has for some time been

51   considered to be associated with the formation of a microemulsion consisting of reverse micellar

52   structures with a polar water core containing ionic species surrounded by a layer of extractant

53   molecules.[9]

54   A number of studies have investigated the process of third phase formation in terms of phase

55   boundaries, mainly studying the limiting organic concentration (LOC), defined as the threshold metal

56   and acid concentrations in the organic phase at which phase splitting occurs. For a more sophisticated

57   treatment of this phase behaviour, we refer to the research of Bauer et al.[10] Third phase formation in

58   extraction of actinides by neutral organophosphorus extractants, including phase boundaries and

59   factors affecting the process of phase splitting, has been thoroughly reviewed.[11] Investigation of the

60   organic phase speciation of neptunium and plutonium in relation to the process of third phase

61   formation has been conducted and the third phase boundaries have been reported.[12] The phenomenon

62   of phase splitting during the extraction of plutonium with TBP in n-dodecane from nitric acid has

63   been studied using small angle neutron scattering (SANS), which indicated that TBP in contact with

64   aqueous phase containing nitric acid and plutonium forms small reverse micelles incorporating three

65   to five TBP molecules. [6] The third-phase formation during the extraction of thorium nitrate from

66   solutions with near-zero free acidity by 1.1M solutions of tri-n-butyl phosphate (TBP) and tri-n-amyl

67   phosphate (TAP) in n-octane, n-decane, n-dodecane, n-tetradecane, and n-hexadecane have been

68   studied and it was found the difference in solute concentrations and density between the third phase

69   and the diluent-rich phase, as well as the ratio of the volume of diluent-rich phase to that of the third

70   phase, can be treated as indices of the third-phase formation tendency.[13]

71   Some mineral acids cause third phase formation with TBP dissolved in aliphatic organic solvents even

72   in the absence of metal ions. For example, the phase splitting phenomenon has been observed at very

73   high nitric acid concentrations in the system HNO_3-TBP in cases when long-chain aliphatic solvents

74   such as n-dodecane are used as TBP diluents.[9] Similarly, the extraction of sulfuric acid by tri-butyl

75   phosphate-kerosene solutions results in three-phase formation at H_2SO_4 concentrations from 6.8 to

76   16 M, independent of the initial TBP concentration.[14] The tendency towards third phase formation of

77   inorganic acids with 0.73 M TBP dissolved in n-octane in terms of decreasing LOC values was found

78   to decrease in the order: $HClO_4 > H_2SO_4 > HCl > H_3PO_4 > HNO_3$.[15] This ordering has since been put

79   on a quantitative basis. [2-4] A considerable amount of research has been devoted to its relationship

80   with the Hofmeister series and we refer to references [11-13] for recent work in this area. Third phase

81   formation in the system HCl/TBP/n-octane system was found to involve the simultaneous extraction

82   of large amounts of water, bringing about organic phase splitting when the equilibrium HCl

83   concentration in the aqueous phase becomes higher than 7.6 M. [19] The extraction by 1.1M tributyl

84   phosphate in n-dodecane of perchloric and nitric acid was found to result in the formation of third

85   phase in solutions with initial aqueous acidic concentration exceeding 2M $HClO_4$ or 15M HNO_3. [20]

86   Based on small-angle X-ray (SAXS) and SANS evidence, the higher potential of perchloric acid for

87   phase splitting the formation of third phase was attributed to the higher polarity of the perchlorate

88   anion, which leads to more effective attractive interaction in the polar cores of the micellar structures.

89   The phenomenon of phase splitting and formation of third phase occurs not only for TBP but across a

90   range of neutral organo-phosphorous extractants when dissolved in long-chain non-polar, aliphatic

91   solvents such as n-dodecane. Such extractants include TBPO, Octyl(Phenyl)-N,N-Diisobutyl

92   Carbamoyl Methyl Phosphine Oxide (CMPO) and Dihexyl N,N-Diethyl Carbamoyl Methyl

93   Phosphonate (DHDECMP). The third-phase formation tendency of DHDECMP varies across

94   inorganic acids in the order $HClO_4 > HNO_3 > HCl > H_2SO_4$.[21] SANS studies suggest that the process

95   of third-phase formation is driven by the formation of DHDECMP·HNO_3 reverse micelles in the

96   diluent phase. After phase separation the size of the aggregates in the third phase was found to be

97   significantly smaller compared to those present when approaching the LOC, with the size of the

98   entities in the heavy phase larger than in the light organic phase. [21]

99   The exact molecular structure and composition of the third phase entities remains unknown. In a

100   recent study, simulation of the behaviour of TBP in the organic phase was carried out, with results

101   suggesting that TBP self-assembles into a bi-continuous phase characterised by filamentous chains of

102   TBP molecules formed by interaction of the oxygen and phosphorous moieties of adjacent TBP

103   molecules. Formation of a molecular micro-emulsion structure was proposed, in which the filaments

104   form a network.[22] The forcefield used in this study, however, overestimated the polarity of the TBP

105   molecules [23] and simulation results using a higher quality forcefield are presented later in this article.

106   Suffice it to state here that these later studies also revealed a micro-emulsion structure rather than

107   reverse micelles. The process of organic phase splitting for several inorganic acids (HNO_3, $HClO_4$,

108   H_2SO_4, and H_3PO_4) extracted with TBP in n-octane was investigated by SANS, which provided

109   evidence for the existence of reverse micelles with diameters from 15 to 22 Å, with polar core

110   diameters ranging from 10 to 15 Å.[24] For the extraction of HCl by TBP dissolved in n-octane the

111   formation of reversed micelles with a maximum TBP aggregation number of 7 and a diameter of 19 Å

112   has been reported.[24] An FTIR spectroscopy study of the system HNO_3/TBP/octane identified two

113   structures, $TBP \cdot HNO_3$ and $TBP \cdot 2HNO_3$.[25] The two nitric acid molecules in the hemi-solvate

114   structure are spectroscopically inequivalent in the vibrations of the P=O bond, which led to the

115   conclusion that the predominant structure of $TBP \cdot 2HNO_3$ involved hydrogen-bonded dimers of

116   HNO_3, with only one of the HNO_3 molecules attached to TBP.[25]

117   In addition to the SANS and SAXS studies already mentioned, other studies with these techniques

118   indicated the formation of large aggregates and reversed micelles in the heavy organic layer. [26-30]

119   Specifically for the HNO_3-TBP system SAXS/SANS indicated that organic phases of TBP in

120   equilibrium with acid solutions contains reverse micelles containing aggregates of 2 to 5 TBP

121   molecules assembled around an aqueous polar core.[31]

122   The present gravimetric and spectroscopic study of the HNO_3/TBP/n-dodecane system was performed

123   to examine third phase formation in this system more systematically and in more detail, particularly to

124   generate additional information on the stoichiometry and the structure of the solvates in the third and

125   organic phases. Shedding light on phase formation in the HNO_3/TBP/n-dodecane system is essential

126   for better understanding more complex extraction systems, and is relevant to the industrial scale

127   reprocessing of spent nuclear fuel.

128

129   **EXPERIMENTAL**

130   **Materials**

131   All reagents were analytical grade. Tri-n-butyl phosphate (Fisher Scientific, 99% purity, density

132   0.979 g ml^{-1}) was used as supplied without any further treatment. Anhydrous n-dodecane (99%,

133   Sigma Aldrich) was used as a solvent for TBP solutions. Perchloric acid 70% (Merck) and 1 M NaOH

134   in methanol (Fisher Scientific) were used for the determination of TBP and HNO_3 concentrations,

135   respectively. All aqueous acidic solutions were prepared using 65% HNO_3 (Sigma Aldrich), 37% HCl

136   (Acros Organics) and 70% $HClO_4$ (Merck). Deionised water (18.2 MΩ·cm) was obtained using a

137   Milli-Q water purification system.

138

139   **Methods**

140   Batch extraction experiments were carried out by mixing 5 ml of acidic solution containing HNO_3,

141   HCl or $HClO_4$ at various concentration levels with an equal volume of 1.1 M (30% by volume) TBP

142   dissolved in n-dodecane. Aqueous and organic samples were placed in 12 ml screw-cap polystyrene

143   centrifuge tubes and intensively shaken for at least 10 min, then positioned upright for several hours

144   to obtain equilibrium and allow phases to separate. As a next step, aliquots of the aqueous, organic

145   and third phases were withdrawn with a 1000 µl Eppendorf pipette (max. error 0.35%) for further

146   analysis. Mass densities were determined by measuring the weight of 1 ml aliquots on an Ohaus

147   Galaxy 160D analytical balance with sensitivity of 10^{-4} g.

148   HNO_3 equilibrium concentrations in organic and third phase samples were determined by direct

149   titration of aliquots with standardised 1 M NaOH solution in methanol using 1% phenolphthalein in

150   ethanol as an indicator. The values reported below represent averages of three consecutive titration

151   measurements. TBP equilibrium concentrations in third phase aliquots were determined

152   volumetrically, determining the volume of the third phase formed by equilibrating the sample with an

153   equal volume of 10 M $HClO_4$. The method requires calibration, conducted by measuring the exact

154   volume of the third phase formed in a number of solutions with known TBP concentration, as

155   described elsewhere.[29, 21] For samples that did not form a third phase, the concentration of TBP in the

156   organic phase was considered to be equal to the initial one, based the negligible TBP solubility in

157   aqueous media. Equilibrium water content in the organic and third phase samples was measured by

158   coulometric titration method using a C20 Compact Karl Fischer coulometric titrator (Mettler-Toledo

159   Inc.).

160   Infrared spectra of organic and third phase samples were recorded using a Nicolet iS10 FT-IR

161   spectrometer (Thermo Scientific). The ^{31}P NMR spectroscopy of organic and third phase samples in 5

162   mm PTFE NMR tubes was performed using a B400 Bruker AVANCE III NMR spectrometer

163   operating at 161.91 MHz. All spectroscopic measurements were carried out at room temperature.

164   Molecular Dynamics Simulations were performed for an organic phase and a third phase using the

165   experimentally determined compositions shown in Table 1. Simulations were performed using the

166   GROMACS package [32-34] at a pressure of 1 bar and a temperature of 298.15 K, using the Parrinello-

167   Rahman barostat [35, 36] and Nosé-Hoover thermostat.[37, 38] The number of TBP, n-dodecane, HNO_3

168   and H_2O molecules were 278, 1267, 255 and 30 respectively for the organic phase, and were 597,

169   711, 1197 and 293 respectively for the third phase. The time step was 1 fs. The systems were

170   equilibrated for 10 ns and the results quoted were averaged over runs of 10 ns. The force field used

171   was the OPLS-2005 [39], where the partial charges on TBP were optimised. [23]

172

173   **RESULTS AND DISCUSSION**

174

175   **Third phase boundaries**

176   In order to study the concentration boundaries of the third phase formation, extraction experiments

177   were conducted by equilibrating equal volumes of nitric acidic solutions with 1.1 M tri-n-butyl

178   phosphate dissolved in n-dodecane. Mass densities of the aqueous and both organic phases were

179   measured as a function of initial HNO_3 concentration, which was in the range between 1.1 and 15.8 M

180   as shown in Fig. 1.

181

182   **Figure 1.** Density of aqueous, organic and third phase in the system HNO_3-1.1 M TBP / n-dodecane

183   as a function of the initial HNO_3 concentration in the aqueous phase

184

185   From the results given in Fig. 1, it can be seen that the aqueous phase density depends linearly on the

186   initial HNO_3 concentration and reaches a maximum value of 1.46 g·ml^{-1} for the sample containing

187   15.8 M initial HNO_3. A two phase region exists below initial HNO_3 concentration of 15 M. Beyond

188   that point the organic phase splits forming a three phase region; 15 M initial HNO_3 appears to be the

189   threshold value for phase splitting. In the two phase region, the organic phase density remains steady

190   in the range between 0.85 and 0.90 g·ml^{-1}. After the threshold concentration, a third phase is formed,

191   causing a decrease in the organic phase density from 0.90 to 0.85 $g \cdot ml^{-1}$ while the third phase density

192   increased from 0.90 to 1.0 $g \cdot ml^{-1}$. The light organic phase after the splitting contains mainly diluent,

193   while HNO_3 and TBP are concentrated in the heavy organic phase, which explains the differences in

194   the phase densities. The limiting density of the aqueous phase corresponding to the phase splitting

195   threshold is approximately 1.43 $g \cdot ml^{-1}$ or 15 M initial HNO_3 concentration. These values are

196   significantly higher compared to the limiting aqueous density of the HNO_3 phase in case of 0.8 M

197   DHDECMP in n-dodecane, which was found to be 1.03 $g \cdot ml^{-1}$, corresponding to 1.1 M initial aqueous

198   HNO_3 concentration.[21] This indicates that TBP is more resistant towards phase splitting and the

199   formation of third phase compared to other neutral organophosphorous extractants such as

200   DHDECMP.

201

202   **Effect of different acids**

203   In a separate series of measurements the occurrence of third phase in systems containing HCl, HNO_3

204   or $HClO_4$ mixed with TBP was studied and the phase densities were determined by mixing 5 ml of the

205   acidic solution with an equal volume of 1.1 M TBP in n-dodecane. In order to investigate the effect of

206   changing the mineral acids the differences between the densities of the heavy and light organic phases

207   for these three systems were determined at initial acid concentrations immediately higher than the

208   LOC (Fig. 2).

209

210   **Figure 2.** Equilibrium density of aqueous, organic and third phase for systems containing HCl, HNO_3

211   and $HClO_4$ with 1.1 M TBP in n-dodecane. The data for each system refer to an initial acid

212   concentration immediately higher than that corresponding to the LOC.

213

214   The density difference between the light and heavy organic phases decreased in the following order:

215    $HClO_4$/TBP > HCl/TBP > HNO_3/TBP. Density differences have previously been considered as an

216   indicator for the tendency to form a third phase.[40] Therefore, based on the experimental results

217   presented in Fig. 2, it can be concluded that $HClO_4$ has the strongest tendency to form third phase

218 with TBP, followed by HCl and HNO_3. In line with this, a previous study concluded that the $HClO_4$

219 system is characterised by much stronger water transfer into the organic phase than for H_3PO_4 and

220 HNO_3.[24] The potential for the formation of third phase during the extraction of inorganic acids by

221 TBP appears to be associated with the acidity strength of the acids, with the pK_a values following the

222 order $HClO_4 > HCl > HNO_3$. This suggests that a better ability to transfer protons may stabilise a

223 more extensive water network solvating the acid in the organic matrix, and thus stabilising the third

224 relative to the organic phase. Again we note the similarity of these results with those published for

225 diamides and it is likely that the same molecular mechanisms are involved. [41] Furthermore, it has

226 been reported that the acid strength order applies only to monoprotic acids. Chiarizia and Briand[15]

227 have demonstrated that if one considers also H_2SO_4 and H_3PO_4, the pKa values do not follow the

228 tendency to phase splitting, which indicates that third phase formation is a more complex

229 phenomenon.

230

231 **Equilibrium TBP, HNO_3 and H_2O concentrations**

232 The equilibrium nitric acid concentrations in both organic and third phase samples with initial

233 aqueous HNO_3 concentration ranging from 1.1 to 15.8 M and initial organic TBP concentration of 1.1

234 M were determined by direct titration of phase aliquots with standard NaOH solution in methanol.

235 The results reveal an increase of the equilibrium HNO_3 levels in the organic phase (Fig. 3), from

236 negligible up to 1.1 M as a function of the initial HNO_3 concentration. The equilibrium nitric acid,

237 water and TBP concentrations, measured in the organic and third phases of systems with highest

238 initial aqueous nitric acid loading of 15.8 M are summarised in Table 1.

239

240 **Figure 3.** Equilibrium HNO_3, TBP and H_2O concentrations in the organic and third phase vs. the

241 initial aqueous HNO_3 concentration.

242

243 The equilibrium organic HNO_3 concentration sharply decreases when the third phase formation

244 boundary is crossed (Fig. 3). It is noteworthy that within the two phase region the equilibrium HNO_3

245   concentration in the organic phase never exceeds the TBP concentration of 1.1 M in the organic

246   phase. This value is exceeded in the third phase that appears at higher HNO_3 concentrations, in which

247   a maximum value of 3.2 M is reached (Fig. 3).

248   A similar trend is evident for the equilibrium molar concentration of H_2O in the organic and third

249   phase samples as determined by Karl Fischer titration (Table 1 and Fig. 3). It can be seen that the

250   distribution of H_2O in the system HNO_3/TBP/n-dodecane mirrors the extraction behaviour of HNO_3,

251   indicating that HNO_3 extraction is accompanied by water transfer from the aqueous to the organic

252   phase. In the absence of third phase formation, the fraction of H_2O transferred to the organic phase is

253   relatively small and increases steadily from 0.17 to 0.24 M as the initial HNO_3 concentration is

254   increased. Once the LOC threshold value is exceeded the majority of the organic phase H_2O

255   molecules are transferred to the third phase, as evident through a decrease of the H_2O content in the

256   organic phase by approximately an order of magnitude.

257   Taking into account that TBP solubility is negligible in the aqueous phase, the equilibrium

258   concentration of TBP in the organic phase of the two-phase systems can be assumed to be equal to the

259   initial TBP concentration. For the three-phase systems, the concentration of TBP in the light organic

260   phase was determined by measuring the volume of the heavy organic phase produced by equilibrating

261   of 5 ml aliquot of the organic phase with an equal volume of 10 M $HClO_4$, as described in the

262   Experimental section. Results indicate that TBP is significantly more concentrated in the third phase

263   compared to the light organic phase. In summary, our compositional analysis indicates that the third

264   phase is enriched in H_2O, HNO_3 and TBP relative to the organic phase, which is depleted in these

265   compounds and mainly contains solvent.

266

267   **Table 1.** Equilibrium concentrations of H_2O, HNO_3 and TBP in the organic and third phases with

268   initial aqueous HNO_3 concentration of 15.8 M

269

270　Based on the stoichiometric data given in Table 1, the equilibrium concentration of TBP in the

271　organic phase appears to be approximately equal to the sum of nitric acid and water equilibrium

272　concentrations:

273　$$[TBP]_{org} = [HNO_3]_{org} + [H_2O]_{org}$$

274

275　The water concentration is a fraction (approximately 12%) of the HNO_3 concentration. This suggests

276　that the main species in the organic phase is the mono-solvate $TBP \cdot HNO_3$, perhaps accompanied by

277　monohydrate $TBP \cdot H_2O$ or the ternary species $TBP \cdot HNO_3 \cdot H_2O$.

278　The equilibrium concentration of HNO_3 in the third phase was twice higher than the equilibrium TBP

279　concentration:

280

281　$$[HNO_3]_{3rd} = 2[TBP]_{3rd}$$

282

283　This stoichiometric ratio suggests that the predominant species in the third phase is the hemi-solvate

284　$TBP \cdot 2HNO_3$. Adding a second HNO_3 molecule to the mono-solvate $TBP \cdot HNO_3$ would increase the

285　polar character of the assemblies, thus decreasing solubility of the species in neutral organic solvent

286　and facilitating the formation of the third phase, in which a higher concentration of water can stabilise

287

288　**^{31}P NMR spectroscopy**

289　Two structurally different models for the third phase $TBP \cdot 2HNO_3$ hemi-solvates have been suggested

290　in the literature with the main being the exact location where the second HNO_3 molecule is bound to

291　the existing $HNO_3 \cdot TBP$ mono-solvate molecule. The second HNO_3 molecule could be directly

292　attached to the P=O group of the tributyl phosphate forming a parallel HNO_3 structure.[42] Other

293　studies indicated that the second HNO_3 molecule is linked to the solvate by a hydrogen bond between

294　the two HNO_3 molecules, forming a chain $TBP \cdot HNO_3 \cdot HNO_3$ structure.[25] In an attempt to shed

295　additional light on this issue and to determine the structures of $TBP \cdot HNO_3$ solvates, a ^{31}P-NMR

296　characterisation of both organic and third phase samples was performed (Fig. 4).

11

297

Figure 4. ^{31}P-NMR spectra of organic (left) and third phase samples (right) of 16 M HNO$_3$-1.1 M

TBP/n-dodecane system

300

The formation of chemical and hydrogen bonds as well as rearrangements and modifications of the

partial chemical structure around the phosphorus centres could lead to changes in the electron density

and hence in chemical shifts in the ^{31}P-NMR spectrum. [43] Attaching a second HNO$_3$ molecule

directly to the TBP phosphate group should result in a downfield ^{31}P chemical shift relative to the

organic phase mono-solvate. However, experimental organic and third phase ^{31}P-NMR spectra (Fig.

4) reveal no strong difference, as both spectra consist of a single narrow signal with chemical shifts of

-1.64 and -1.54 ppm, respectively. The relatively narrow peak widths of less than 10 ppm suggest that

the composition of TBP species is rather uniform, with no distribution of chemically distinct

species.[44]

310

Fig. 5. Proposed structure of the third phase TBP·2HNO$_3$ hemi-solvates

312

The lack of significant chemical shift in the third phase ^{31}P-NMR spectrum compared to the spectrum

of the organic phase provides a strong indication that the third phase formation and the addition of an

extra HNO$_3$ molecule to the organic TBP·HNO$_3$ mono-solvates is not associated with the immediate

chemical surroundings of phosphorus moieties in TBP. Therefore, it appears likely that the third phase

solvate structure involves two HNO$_3$ molecules hydrogen-bonded to each other forming a chain

TBP·HNO$_3$·HNO$_3$ structure as shown in Fig. 5.

319

Figure 6. IR spectra of organic phase samples with initial aqueous HNO$_3$ concentration of 2, 4, 6, 8,

10, 12 and 14 M (from bottom to top)

322

Infrared spectroscopy

Organic samples with various initial aqueous HNO_3 concentrations were also analysed using infrared spectroscopy (Figure 6). There is a sharp increase in the intensity of the peaks at 1653 and 1310 cm^{-1} with increasing initial aqueous HNO_3 concentration. These peaks stem from the asymmetric NOO stretching (1700-1620 cm^{-1}) and the symmetric NOO stretching (1330-1280 cm^{-1}).[25, 43] The increase in the intensities of these bands with an increase in aqueous HNO_3 concentration despite the decrease in HNO_3 concentration quantified (figure 3) is due to the increase in mono-solvate TBP·HNO_3 concentration in the organic phase. The broad peak at 3500-3200 cm^{-1} also increased in intensity which corresponds to the O-H stretching band of HNO_3, in line with the higher HNO_3 concentrations in the organic phase (see fig. 3) as a function of aqueous HNO_3 concentration. The intensity of the vibrational bands at 1028 cm^{-1} (P-O-C stretch),[28] related to the TBP concentration together with the triplet at 3000-2800 cm^{-1} (C-H stretch), showed no significant differences indicating that the equilibrium concentrations of TBP and n-dodecane remain constant.

Table 2. Major vibrational bands relevant to the HNO_3-TBP system [25]

The infrared spectra of both organic and third phases with an initial aqueous HNO_3 concentration of 15.1 M were also measured (Fig. 7). Both spectra include identical sets of vibrational bands. The main differences between the organic and third phase IR spectra are in the intensities of some vibrational bands. The third phase spectrum shows higher peak intensities at 1028, 1310, 1653 and 3200-3500 cm^{-1} compared to the organic phase. These higher intensities are in line with the higher concentrations of H_2O, HNO_3 and TBP in the third phase. The intensity of the 3000–2850 cm^{-1} band (C-H stretch) decreases in the third phase spectra, reflecting the fact that the n-dodecane concentration is lower than in the organic phase.

Figure 7. IR spectra of organic vs. third phase samples with initial aqueous HNO_3 concentration of 15.1 M

350

351 **Molecular Dynamics Simulations**

352 In order to obtain structure models for the organic and third phases molecular dynamics simulations[45]

353 were performed for an organic phase and a third phase using the experimentally determined

354 compositions shown in Table 1. Simulation snapshots of the two phases, where for clarity only 2 nm

355 slices are shown, are shown in Figures 8 and 9. While the structures shown are mobile and will flex

356 and bend, the basic topology does not alter with time. We see no evidence of reverse micelles. Instead

357 the structure resembles a bi-continuous emulsion on the molecular scale, with the TBP molecules

358 acting as surfactants. The butyl groups of the TBP are in contact with the dodecane diluent, while

359 polar molecules, such as nitric acid and water, are associated with the polar phosphate groups.

360

361 **Figure 8.** A snapshot of the organic phase system. TBP, HNO_3 and H_2O molecules are represented in

362 yellow, red and blue, respectively; n-dodecane molecules are not shown for clarity

363

364 If we consider the organic phase with a relatively low nitric acid concentration, we observed

365 predominantly monodentate TBP-HNO_3 complexes. At higher nitric acid concentrations,

366 corresponding to the observed third phase composition, we see TBP-HNO_3-HNO_3 complexes, in

367 agreement with the conclusion drawn above from the ^{31}P NMR data. The water molecules are

368 somewhat randomly distributed around the system and while one can occasionally find TBP-HNO_3-

369 HNO_3-H_2O-HNO_3-HNO_3-TBP chains, they are not common. Our belief is that the experimentally

370 observed stoichiometry does not stem from a significant presence of such extended structures.

371

372 **Figure 9.** A snapshot of the third phase system. TBP, HNO_3 and H_2O molecules are represented in

373 yellow, red and blue, respectively; n-dodecane molecules are not shown for clarity

374

375 In addition, the average number of hydrogen bonds between molecule pairs was analysed. The

376 criterion for determining the presence of a hydrogen bond was that the donor-acceptor distance should

377 be no more than 0.35 nm and the acceptor-donor-hydrogen angle should be no more than 30°. The

378 oxygen atoms that have covalent bonds with the hydrogen atoms in the H_2O and HNO_3 molecules

379 were regarded as potential donors and the electronegative atoms that possess a lone electron pair were

380 regarded as potential acceptors. The average numbers of hydrogen bonds between pairs of TBP,

381 HNO_3 or H_2O molecules are shown in Table 3.

382

383 **Table 3.** Average numbers of hydrogen bonds between molecule pairs

384

385 To recap, the numbers of TBP, n-dodecane, HNO_3 and H_2O molecules used in the MD simulations

386 were 278, 1267, 255 and 30 respectively for the organic phase, and 597, 711, 1197 and 293

387 respectively for the third phase.

388 In the light organic phase, the number of TBP·HNO_3 hydrogen bonds is 231 (Table 3), which

389 accounts for 91% of HNO_3 and 83% of TBP molecules. The number of TBP·H_2O hydrogen bonds is

390 33, which accounts for 111% of H_2O and 12% of TBP molecules. Note the 111% here indicates that

391 100% of H_2O molecules are connected with TBP and 11% of these are connected with two TBP

392 molecules. The number of HNO_3·HNO_3 hydrogen bonds is only 4. These results indicate that there

393 are large numbers of TBP·HNO_3 dimers and only a small number of HNO_3-HNO_3 dimers. Hence

394 TBP·HNO_3 is the predominant structure in the light organic phase, in line with the experimental

395 results. In addition, it is very likely that each H_2O molecule forms at least one hydrogen bond with a

396 TBP molecule in the light organic phase.

397 In the third phase, however, the number of TBP·HNO_3 hydrogen bonds is 619, which corresponds to

398 52% of HNO_3 and 104% of TBP molecules. Note the 104% here indicates that 100% of TBP

399 molecules are connected with HNO_3 and 4% of these are likely bidentate species linked to two

400 monodentate HNO_3 molecules. The number of HNO_3-HNO_3 hydrogen bonds is 284, which involves

401 47% of the HNO_3. The number of TBP-H_2O hydrogen bonds only accounts for 31% of H_2O, which is

402 noticeably lower than in the light organic phase. These results could be explained by the formation of

403   bidentate TBP·2HNO$_3$ complexes in the third phase, predominantly TBP-HNO$_3$-HNO$_3$ aggregates,

404   again in line with the ^{31}P NMR results. In addition, the number of HNO$_3$-H$_2$O hydrogen bonds is

405   almost twice the number of H$_2$O molecules, which indicates that one H$_2$O is typically shared between

406   two HNO$_3$ molecules. Hence, HNO$_3$-H$_2$O-HNO$_3$ aggregates may be a common structure in the third

407   phase. A very recent paper [46] also presents the results of molecular dynamics simulations of this

408   system and the hydrogen bonding analysis is broadly in agreement with that given above.

409   Overall, the observed behaviour of the TPB/HNO$_3$/H$_2$O/dodecane system has much in common with

410   oil/water/surfactant systems. The phases we report have similarities with the Winsor-III classification

411   of surfactant micro-emulsion systems [47], where bi-continuous micro-emulsion phases are found.

412   What differentiates our system from most surfactant systems, however, is that we believe we have

413   phase co-existence between two bi-continuous micro-emulsion phases, both of isotropic symmetry.

414   Most Winsor III phase diagram show, instead, co-existence between a bi-continuous and a micellar

415   phase (or a phase of different symmetry). A recent review of surfactant phase behaviour is given by

416   Hyde et al [48] and we note the work of Erlinger [5], which describes the transition of reverse micelles

417   to a bi-continuous structure. It is interesting to note in this context the two level-cut Gaussian random

418   wave representations of the micro-structure of bi-continuous structures [49,50], which show a striking

419   resemblance to the molecular dynamics snapshots shown in Figures 8 and 9. The fact that the majority

420   of water-poor microemulsion systems exhibit bicontinuous structures rather than reverse micelles

421   gives, arguably, extra credence to the results we have presented.

422

423   **CONCLUSIONS**

424   Third phase boundaries of the system the system HNO$_3$-1.1 M TBP/n-dodecane were determined by

425   measuring the phase densities. The formation of third phase occurred when the initial aqueous nitric

426   acid concentration is higher than 15 M. Based on stoichiometric ratio analysis, two different species

427   have been identified in the organic and third phase, mono-solvate TBP·HNO$_3$ and the hemi-solvate

428   TBP·2HNO$_3$, respectively. The ^{31}P-NMR spectra of both organic and third phase have been obtained

429   and no significant differences have been observed, suggesting that the attachment of a second HNO$_3$

430   molecule to the TBP·HNO$_3$ mono-solvate does not affect the chemical state of the phosphorus centres.

431   This indicates that the TBP·2HNO$_3$ solvate structure involves two HNO$_3$ molecules, linked together in

432   a chain of HNO$_3$ dimers in the form of TBP·HNO$_3$·HNO$_3$. Infrared spectra of the organic phase show

433   that an increase in the intensity of the vibrational bands, assigned to O-H (3200-3500 cm^{-1}),

434   asymmetric NOO (1620-1700 cm^{-1}) and symmetric NOO stretches (1280-1330 cm^{-1}) with increasing

435   initial aqueous nitric acid concentration. The intensity of the vibrational bands associated with C-H

436   stretch (2800-3000 cm^{-1}) and P-O-C stretch (1028 cm^{-1}) remain constant. Compared with the organic

437   phase with identical initial aqueous HNO$_3$ concentration, the third phase spectrum shows stronger

438   absorption at 1028, 1310, 1653 and 3200-3500 cm^{-1}, reflecting the fact that the third phase is enriched

439   in H$_2$O, HNO$_3$ and TBP. Molecular dynamics simulation predict structures in accord with the

440   experimentally observed spectroscopic data, indicating inequivalent HNO$_3$ molecules in the third

441   phase. The structures of the organic and third phases are more akin to micro-emulsion networks than

442   distinct, reverse micelles. Similarities with bi-continuous micro-emulsion phases in the Winsor-III

443   classification of surfactant micro-emulsion systems are evident, although the current system appears

444   to be characterised by phase co-existence between two isotropic bi-continuous micro-emulsion

445   phases. The results of our molecular dynamics analysis of the microstructure are in line with previous

446   Gaussian random wave representations of the micro-structure of bi-continuous structures. [49,50]

452

453   **REFERENCES**

454   1. Spent Fuel Reprocessing Options, IAEA-Tecdoc-1587, 2008.

455   2. Dejugnat, C., Berthon, L., Dubois, V., Dourdain, S., Meridiano, Y., Guillaumont, D., Pellet-

456   Rostaing, S., Zemb, T. Liquid-liquid extraction of acids and water by a malonamide: I-Anion

457   specific effects on the polar core microstructure of the aggregated malonamide. Solvent Extr.

458   Ion Exch. 2014, 32, 601-619.

459   3. Dourdain, S., Dejugnat, C., Berthon, L., Dubois, V., Pellet-Rostaing, S., Dufreche, J.F., Zemb,

460   T. Liquid-liquid extraction of acids by a malonamide: II-anion specific effects in the aggregate

461   –enhanced extraction isotherms. Solvent Extr. Ion Exch. 2014, 32, 620-636.

462   4. Dejugnat, C., Dourdain, S., Berthon, L., Dubois, V., Berthon, L., Pellet-Rostaing, S., Dufreche,

463   J.F., Zemb, T. Reverse aggregate nucleation induced by acids in liquid-liquid extraction

464   process. Phys. Chem. Chem. Phys. 2014, 16, 7339-7349.

465   5. Erlinger, C., Belloni, L., Zemb, T., Madic, C. Attractive interactions between reverse

466   aggregates and phase separation in concentrated malonamide extractant solutions. Langmuir

467   1999, 15(7), 2290–2300.

468   6. Plaue, J.; Gelis, A.; Czerwinski, K. Plutonium third phase formation in the 30% TBP/nitric

469   acid/hydrogenated polypropylene tetramer system. Solvent Extr. Ion Exch. **2006**, 24, 271-282.

470   7. Chiarizia, R.; Jensen, M.P.; Borkowski, M.; Ferraro, J.R.; Thiyagarajan, P.; Littrell, K.C.

471   Third phase formation revisited: The U(VI), HNO$_3$–TBP, n-dodecane system. Solvent Extr.

472   Ion Exch. **2003**, 21(1), 1-27.

473   8. Marcus, Y.; Kertes, A.S. Ion Exchange and Solvent Extraction of Metal Complexes; Wiley

474   Interscience: New York, 1969; p. 715.

475   9. Osseo-Asare, K. Aggregation, reversed micelles and microemulsions in liquid-liquid

476   extraction: The tri-n-butylphosphate- diluent- water- electrolyte system. Adv. Colloid

477   Interface Sci. **1991**, 37, 123–173.

478 10. Bauer, C., Baudiun, P., Dufreche, J.F., Zemb, T., Diat, O. Liquid/liquid metal extraction:

479   Phase diagram topology resulting from molecular interactions between extractant, ion, oil and

480   water. Eur. Phys. J. Special Topics **2012**, 213, 225-241.

481 11. Vasudeva Rao, P.R.; Kolarik, Z. A review of third phase formation in extraction of actinides

482   by neutral organophosphorus extractants. Solvent Extr. Ion Exch. **1996**, 14(6), 955-993.

483 12. Plaue, J.; Gelis, A.; Czerwinski, K. Actinide third phase formation in the 1.1M TBP/nitric

484   acid/alkane diluent system. Solvent Extr. Ion Exch. **2006**, 41, 2065-2074.

485   13. Mallick, S.; Suresh, A.; Srinivasan T.G.; Vasudeva Rao, P.R. Comparative Studies on Third-

486   Phase Formation in the Extraction of Thorium Nitrate by Tri-n-Butyl Phosphate and Tri-n-

487   Amyl Phosphate in Straight Chain Alkane Diluents. Solvent Extr. Ion Exch. **2010**, 28, 459-

488   481.

489   14. Fu, X.; Hu, X.P.; Zhang, Z.; Hu, Z.; Wang, D. Three phase extraction study. I. Tri-butyl

490   phosphate-kerosene:H_2SO_4-H_2O extraction system. Colloid Surface A, **1999**, 152, 335-343

491   15. Chiarizia, R.; Briand, A. Third phase formation in the extraction of inorganic acids by TBP in

492   n-octane. Solvent Extr. Ion Exch. **2006**, 24(3), 283-297.

493   16. Leontidis, E. Christoforou, M, Georgiou, C., Delclos, T. The ion-lipid battle for hydratation

494   water and interfacial sites at soft-matter interfaces. Curr. Opinion Coll. Interf. Sci. **2014**, 19,

495   2-8.

496   17. Leontidis, E. Chaotropic salts interacting with soft matter: Beyond the lyotropic series. Curr.

497   Opinion Coll. Interf. Sci. **2016**, 23, 100-109.

498   18. Schwierz, N., Horinek, D., Sivan, U., Netz, R.R. Reversed Hofmeister series- The rule rather

499   than exception. Curr. Opinion Coll. Interf. Sci. **2016**, 23, 10-18.

500   19. Chiarizia, R.; Rickert, P.G.; Stepinski, D.; Thiyagarajan, P.; Littrell, K.C. SANS study of

501   third phase formation in the HCl-TBP-n-octane system. Solvent Extr. Ion Exch. **2006**, 24(2),

502   125-148.

503   20. Nave, S.; Mandin, C.; Martinet, L.; Berthon, L.; Testard, F.; Madic C.; Zemb Th.

504   Supramolecular organisation of tri-n-butyl phosphate in organic diluent on approaching third

505   phase transition. Phys. Chem. Chem. Phys. 2004, 6, 799-808.

506   21. Lohithakshan, K.V.; Aswal, V.K., Aggarwal, S.K. Studies on the third phase formation in

507   DHDECMP/dodecane/HNO_3. Radiochim. Acta **2011**, 99, 179-186.

508   22. Leay, L., Tucker, K., Del Regno, A., Schroeder, S.L.M., Sharrad, C.A., Masters, A.J. The

509   behaviour of tributyl phosphate in an organic diluent. Mol. Phys. **2014**, 112(17), 2203-2214.

510   23. Mu, J., Motokawa. R., Williams. C.D., Akutsu. K., Masters. A.J., A Comparative Molecular

511   Dynamics Study on Tri-n-butyl Phosphate in Organic and Aqueous Environments and its

512   Relevance to Nuclear Extraction Processes. J. Phys. Chem. B, **2016**, 120 (23), 5183-5193.

513   24. Chiarizia, R.; Briand, A.; Jensen, M.P., Thiyagarajan, P. SANS study of reverse micelles

514   formed upon the extraction of inorganic acids by TBP in n-octane. Solvent Extr. Ion Exch.

515   **2008**, 26(4), 333-359.

516   25. Ferraro, J.R.; Borkowski, M.; Chiarizia, R.; McAlister, D.R. FT-IR spectroscopy of nitric acid

517   in TBP/octane solution. Solvent Extr. Ion Exch. **2001**, 19(6), 981-992.

518   26. Chiarizia, R.; Jensen, M.P.; Borkowski, M.; Ferraro, J.R.; Thiyagarajan, P.; Littrell, K.C.

519   SANS study of third phase formation in the U(VI)-HNO$_3$/TBP-n-dodecane system. Sep. Sci.

520   Technol. **2003**, 38(12), 3313-3331.

521   27. Borkowski, M.; Chiarizia, R.; Jensen, M.P.; Ferraro, J.R.; Thiyagarajan, P.; Littrell, K.C.

522   SANS study of third phase formation in the Th(IV)-HNO$_3$/TBP-n-octane system. Sep. Sci.

523   Technol. **2003**, 38(12), 3333-3351.

524   28. Chiarizia, R.; Nash, K. L.; Jensen, M. P.; Thiyagarajan, P.; Littrell, K. C. Application of the

525   Baxter Model for hard-spheres with surface adhesion to sans data for the U(VI)-HNO$_3$, TBP-

526   n-dodecane system. Langmuir, **2003**, 19, 9592-9599.

527   29. Chiarizia, R.; Jensen, M. P.; Rickert, P. G.; Kolarik, Z.; Borkowski, M.; Thiyagarajan, P.

528   Extraction of zirconium nitrate by TBP in n-octane: Influence of cation type on third phase

529   formation according to the ''sticky spheres'' model. Langmuir, **2004**, 20, 10798-10808.

530   30. Plaue, J.; Gelis, A.; Czerwinski, K.; Thiyagarajan, P.; Chiarizia, R. Small-angle neutron

531   scattering study of plutonium third phase formation in 30% TBP/HNO$_3$/alkane diluent

532   systems. Solvent Extr. Ion Exch. **2007**, 25(3), 351-371.

533   31. Shilin, I. V.; Indikov, E. M.; Zhdanov, Yu. F.; Makarov, D. G. Method for determination of

534   TBP in TBP- kerosene mixtures. USSR Patent 114,186, 1958.

535   32. Bekker, H., et al, Gromacs: A parallel computer for molecular dynamics simulations. Physics

536   Computing. **1993**, 92, 252-256.

537   33. Berendsen, H.J., D. van der Spoel, and R. van Drunen, GROMACS: A message-passing

538   parallel molecular dynamics implementation. Comput. Phys. Commun.. **1995**, 91, 43-56.

539   34. Van Der Spoel, D., et al., GROMACS: fast, flexible, and free. J. Comput. Chem. **2005**, 26,

540   1701-1718.

541   35. Parrinello, M. and A. Rahman, Polymorphic transitions in single crystals: A new molecular

542   dynamics method. J. Appl. Phys. **1981**, 52, 7182-7190.

543   36. Nosé, S. and M.L. Klein, Constant pressure molecular dynamics for molecular systems. Mol.

544   Phys. **1983**, 50, 1055-1076.

545   37. Nosé, S., A unified formulation of the constant temperature molecular dynamics methods. J.

546   Chem. Phys. **1984**, 81, 511-519.

547   38. Hoover, W.G., Canonical dynamics: equilibrium phase-space distributions. Phys. Rev. A.

548   **1985**, 31, 1695.

549   39. Banks, J.e.a., Integrated modeling program, applied chemical theory (IMPACT). J. Comput.

550   Chem. **2005**, 26, 1752-1780.

551   40. Stoyanov, E.S., Mihailov, V.A., Chekmarev, A.M., Chizhevskaya, S.V. The composition and

552   structure of the associates of nitric acid extracted from its concentrated aqueous solutions by

553   100% TBP. Russ. J. Inorg. Chem. **1990**, 35, 821-826.

554   41. Qiao, B., Ferru, G., De la Cruz, M.O., Ellis, R.J. Molecular origins of mesoscale ordering in a

555   metalloamphiphile phase. ASC Cent. Sci. **2015**, 1, 493-503.

556   42. Uetake, N. Chemical state detection of dibutyl phosphate using ^{31}P NMR chemical shift

557   change. Can. J. Chem. **1991**, 69, 322-326.

558   43. Sarsfield, M.J., Taylor, R.J., Maher, C.J. Neptunium(V) disproportionation and cation-cation

559   interactions in TBP/kerosene solvent. Radiochim. Acta **2007**, 95, 677-682.

560   44. Urtake, N. Precipitation formation of zirconium dibutyl phosphate complex in Purex process.

561   J. Nucl Sci. Technol. **1989**, 26(3), 329-338.

562   45. Rapaport, D.C., The art of molecular dynamics simulation. 2004: Cambridge university press.

563   46. Servis, M.J., Wu, D.T., Braley, J. Network analysis and percolation transition in gen bonded

564   clusters: Nitric acid and water extraction by tributyl phosphate. Phys. Chem. Chem. Phys.

565   2017, DOI: 10.1039/C7CP01845B.

566   47. Winsor, P.A. Hydrotropy, solubilisation and related emulsification processes. Trans Faraday

567   Soc., **1948**, 44, 376–398.

568   48. Hyde, S.H. et al. 1997. Colloids and Surfaces A, 129-130, 435-454.

569   49. Duvail, M., Dufreche, J.F., Arleth, L., Zemb, T. Mesoscopic modelling of frustration in

570   microemulsions. Phys. Chem. Chem. Phys. **2013**, 15, 7133-7141.

571   50. Teubner, M. Level surfaces of Gaussian random fields and microemulsions. Europhys. Lett.

572   **1991**, 14(5), 403-408.

573

574

23

597 **Figure 9.** The snapshot of the third phase system. TBP, HNO_3 and H_2O molecules are represented in

598 yellow, red and blue, respectively; n-dodecane molecules are not shown for clarity

599 **FIGURES AND TABLES**

600

601 **Table 1.** Equilibrium concentrations of H_2O, HNO_3 and TBP in the organic and third phases with

602 initial aqueous HNO_3 concentration of 15.8 M

Compound	Concentration in the organic phase, M	Concentration in the third phase, M
H_2O	0.08	0.77
HNO_3	0.68	3.15
TBP	0.74	1.57

603

604

605   **Table 2.** Major vibrational bands relevant to the HNO_3-TBP system [25]

Assignment	Frequency, cm^{-1}
P-O-C stretch	1028
P=O stretch	1282
NOO symmetric stretch	1304
NOO asymmetric stretch	1627

606

607

608

609 **Table 3.** Average numbers of hydrogen bonds between molecule pairs

Molecule pair	The light organic phase	The third phase
TBP – HNO_3	231	619
TBP – H_2O	33	89
HNO_3 – HNO_3	4	284
HNO_3 – H_2O	28	584
H_2O – H_2O	4	20

610

611
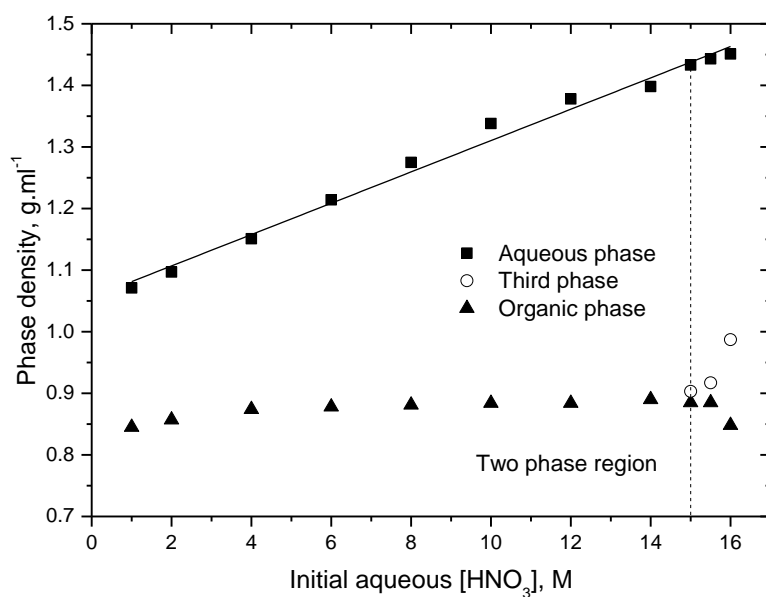
612

613 **Figure 1.** Density of the aqueous, organic and third phases in the system: HNO_3-1.1 M TBP / n-

614 dodecane as a function of the initial HNO_3 concentration in the aqueous phase

615

616
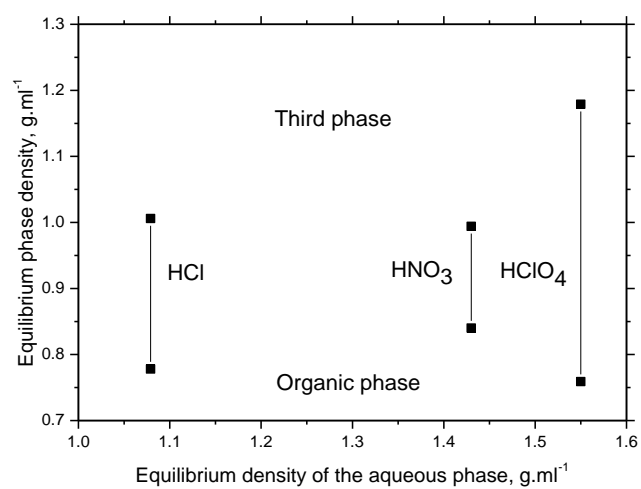
617

Figure 2. Equilibrium density of aqueous, organic and third phase for systems containing HCl, HNO$_3$

and HClO$_4$ with 1.1 M TBP in n-dodecane. The data for each system refer to an initial acid

concentration immediately higher than that corresponding to the LOC.

617
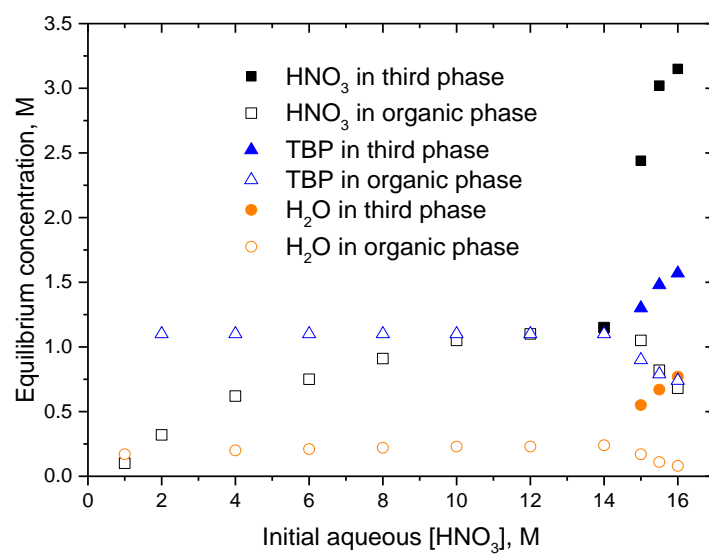
618

619

620

621

622

623

Figure 3. Equilibrium HNO$_3$, TBP and H$_2$O concentrations in the organic and third phase vs. the

625   initial aqueous HNO$_3$ concentration

626

627

628

629

630

631

632

633

634

635

636

637

638

639

640

641

642 **Figure 4.** ^{31}P-NMR spectra of organic (left) and third phase samples (right) of 16 M HNO$_3$-1.1 M
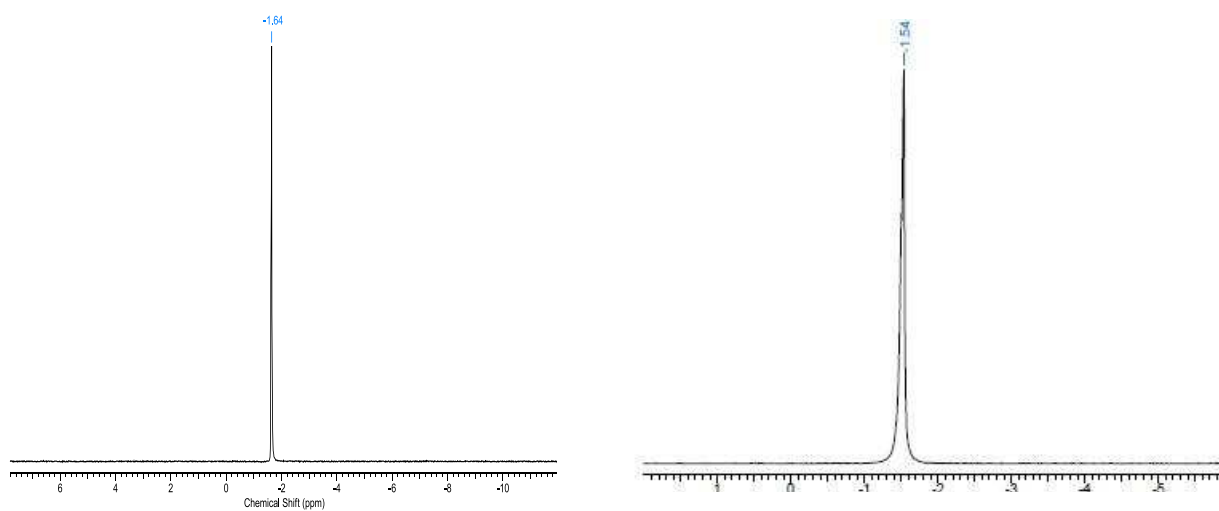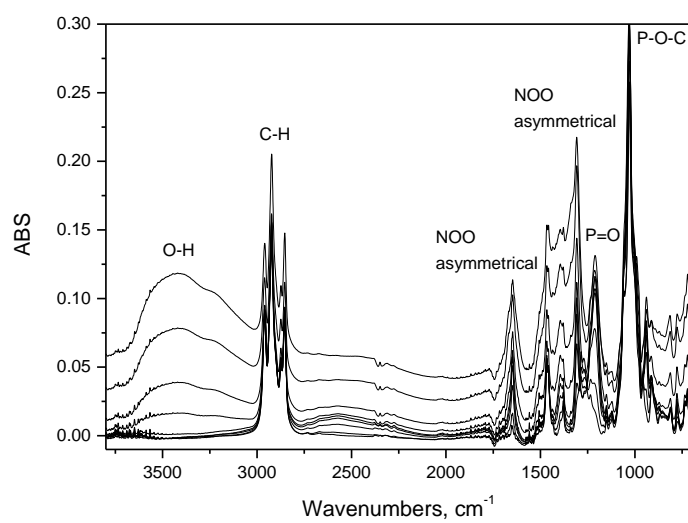
643 TBP/n-dodecane system

644

645

646

647
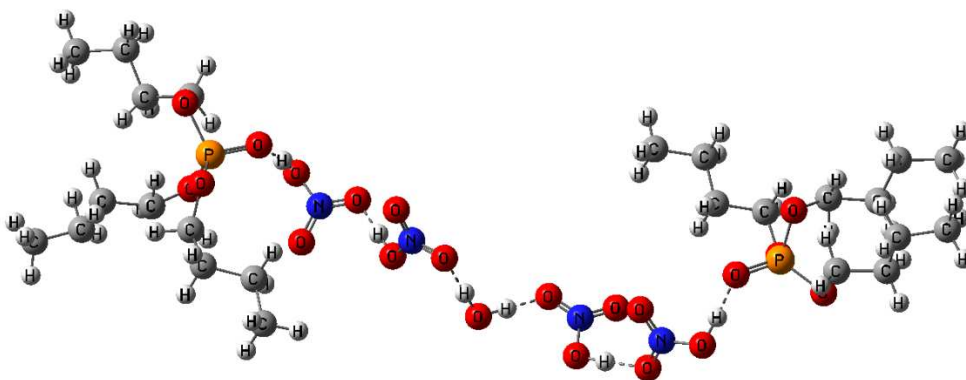
648

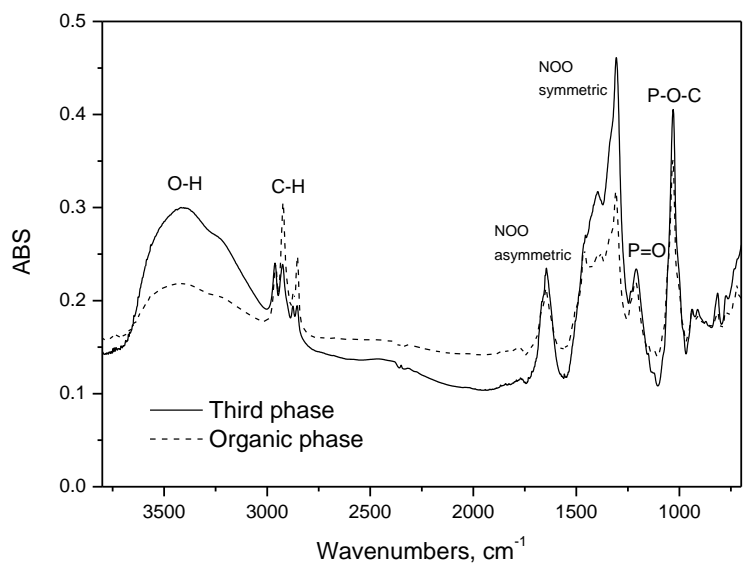649 **Fig. 5.** Suggested structure of the third phase TBP·2HNO₃ hemi-solvates

650

651

652

Figure 6. IR spectra of organic phase samples with initial aqueous HNO_3 concentration of 2, 4, 6, 8, 10, 12 and 14 M (from bottom to top)

655

656

657

658   **Figure 7.** IR spectra of organic vs. third phase samples with initial aqueous HNO_3 concentration of
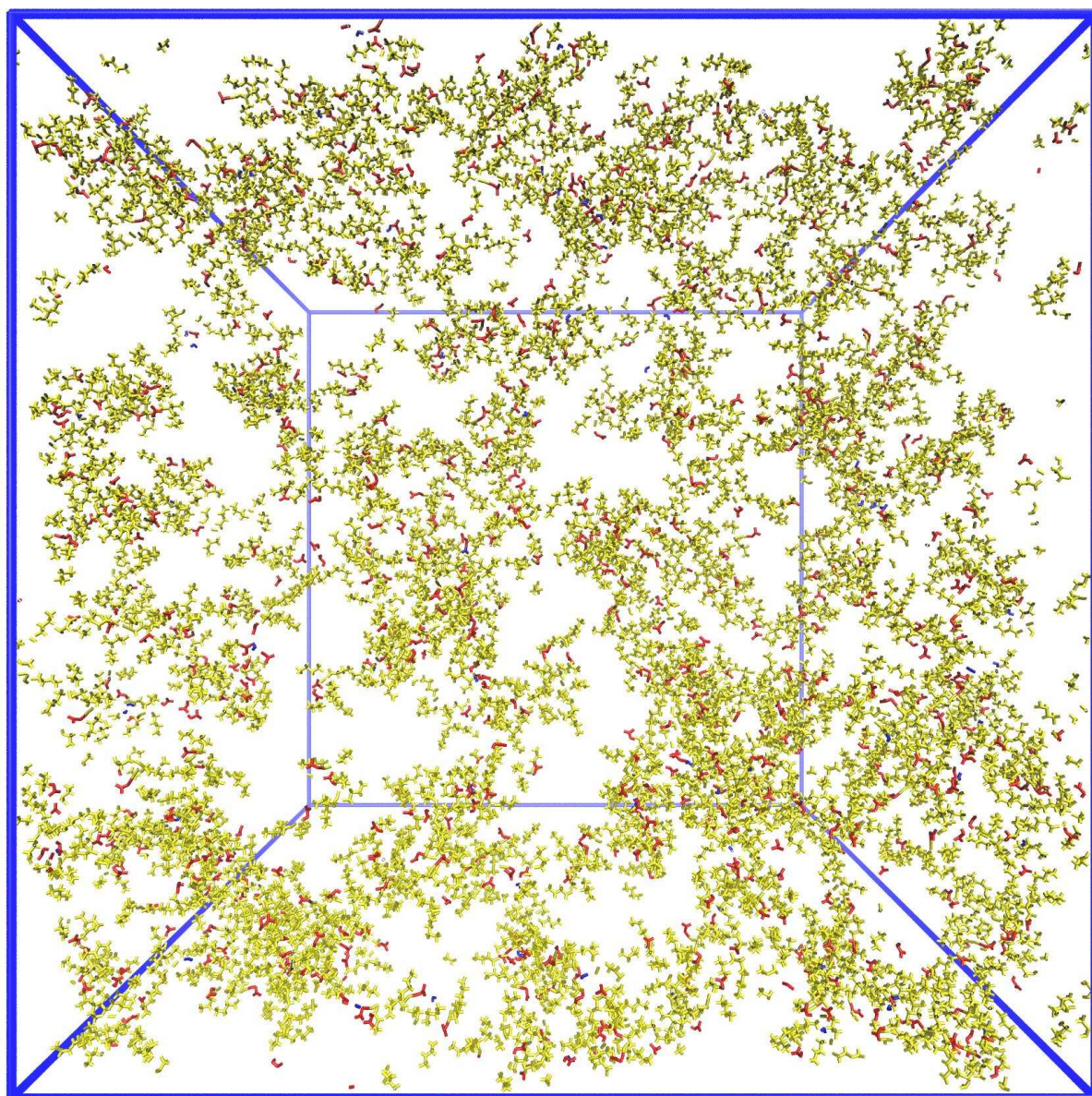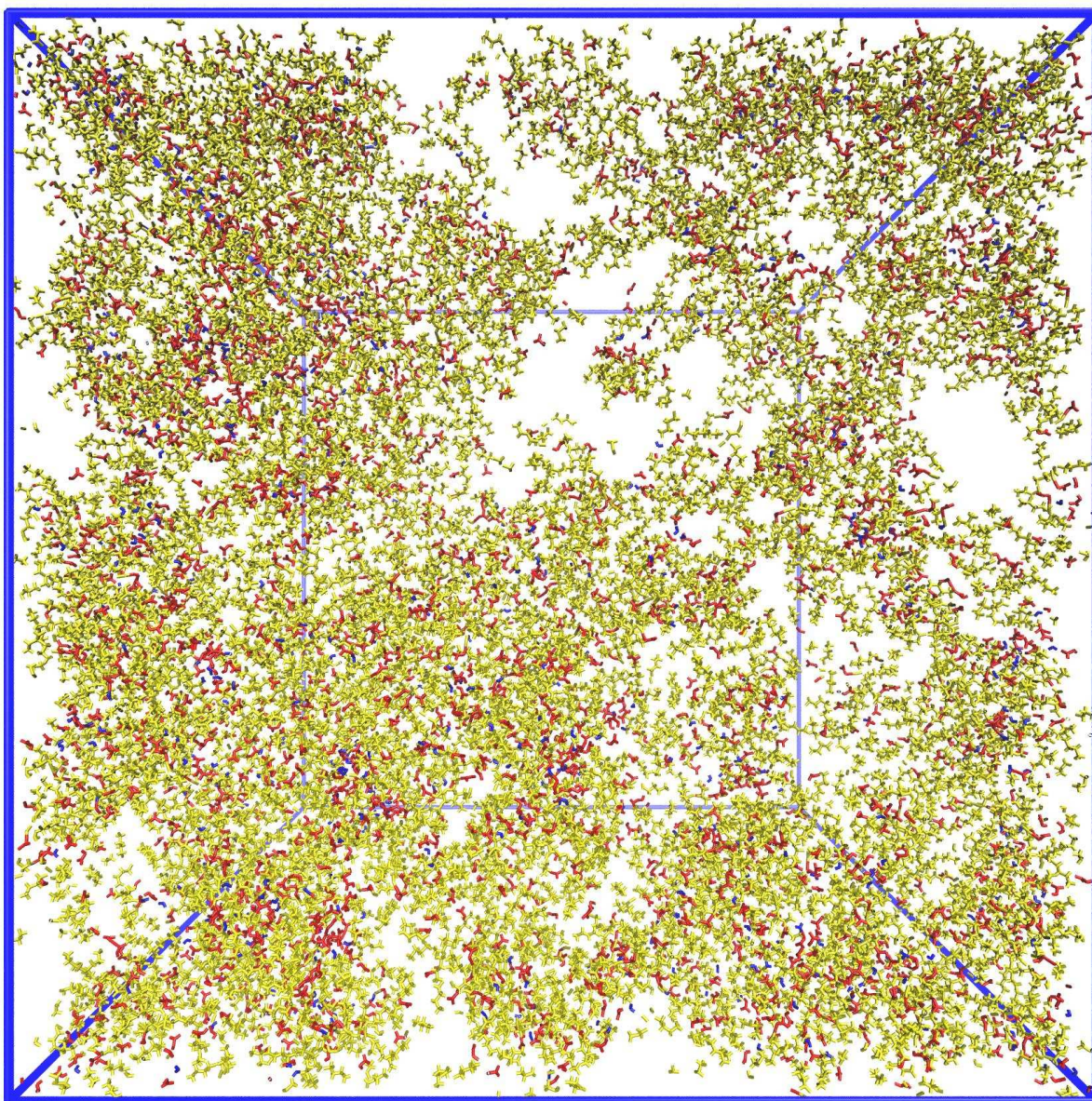
659   15.1 M

660

661

662

663

664

Figure 8. The snapshot of the organic phase system. TBP, HNO_3 and H_2O molecules are represented in yellow, red and blue, respectively; n-dodecane molecules are not shown for clarity

665

666

667

668

669

670

671   **Figure 9.** The snapshot of the third phase system. TBP, HNO_3 and H_2O molecules are represented in

672   yellow, red and blue, respectively; n-dodecane molecules are not shown for clarity

673